Applied Physics B (2021) 127:163
https://doi.org/10.1007/s00340-021-07712-8

Applied Physics B
Lasers and Optics

Long-period fiber grating embedded in polymer structure for deformation monitoring

Renato Luiz[1] · Deivid Campos[1] · Felipe de Souza Delgado[1,2] · Alexandre Bessa dos Santos[1]

Received: 30 July 2021 / Accepted: 31 October 2021 / Published online: 12 November 2021

Abstract
We propose a strain sensor based on a long-period fiber grating (LPFG) packaged in a 3D-printed structure made of polymer material. The proposed sensing structure was fabricated using a commercially available 3D printer by embedding a bare LPFG sensor inside the polymer material during the printing process. The raw material used for the fabrication of the polymer structure was Polylactic Acid (PLA). We experimentally investigated the strain-dependent spectral response of the produced sensor by observing the transmitted spectral profile. Finally, the results showed that a linear strain sensitivity of − 4.6 pm/με with the range of 0–1000 με was achieved, therefore indicating that the proposed sensing device is suitable for strain deformation measurement.

1 Introduction

In recent years, there has been an increasing demand of compact, portable, lightweight and high-performance sensors and sensing technologies. Therefore, stimulating the research and industrial communities towards the development of innovative sensing concepts [1]. In this context, the 3D printing technology is attracting increasing attention in applications of optical fiber sensors coatings, packaging and smart materials [2–4], due to its advantages of low cost, flexibility, high repeatability and facility to fabricate structures with embedded optical fiber sensors [5]. Furthermore, the 3D printing consists of using plastic material to create the three-dimensional desired packaging structure [6], which can be fabricated using different polymer materials. The most common plastics used in 3D printing are polylactic acid (PLA), acrylonitrile butadiene styrene (ABS), polycarbonate (PC), and thermoplastic polyurethane (TPU) [7].

The fiber gratings are found among the most popular devices used in optical fiber sensing. There are two main types of grating sensors: the short-period gratings, also called fiber Bragg gratings (FBG), and transmission gratings, also referred to as long-period fiber gratings (LPFG). The encapsulation of these sensors into 3D-printed plastic material produces a compact and robust sensing structure, which enhances the protection of the optical fiber [8–10]. Recently, FBG sensors packaged by 3D printing technology have been explored in different sensing applications. For example, Fang et al. [11] reported the application of embedded FBG sensors in a cantilever to investigate the strain variation while it was loaded. In what concerns the performance and sensing characteristics of the packed sensors, Leal-Junior et al. [12] reported FBGs embedded in 3D-printed sensing pads using ABS material and investigated the impact of infill density on sensitivity and dynamic range in force sensors. Whereas Yan et al. [13] systematically analyzed the influence of packaging scheme using PLA as raw material on the sensing characteristics of the packaged FBG. However, to the best of the authors' knowledge, the application of LPFGs embedded in a 3D-printed polymer structure in sensing fields have not been explored and presented in literature before.

In this work, we have developed a LPFG-embedded strain sensor by embedding a bare LPFG sensor inside polylactic acid (PLA) polymer material using a commercially available 3D printer. The performance and spectral characteristics of the developed sensor were examined before and after embedment for strain varying from 0 to 1000 με. A benefit of the proposed sensor configuration is that the LPFG is immobilized and bonded inside the PLA structure. Therefore, improving the reliability of the sensor for repeated use over time. Finally, the experimental results indicate that the

✉ Felipe de Souza Delgado
felipedelgado@cefetmg.br

[1] Electrical Engineering Department, Federal University of Juiz de Fora, Juiz de Fora, MG, Brazil

[2] Electrical Department, CEFET-MG, Nepomuceno, MG, Brazil

embedding has a significant impact on the strain response of the sensor, therefore, enhancing the performance of the sensor.

2 Operating principle and fabrication

The attenuation bands of a LPFG, which are located at specific resonance wavelengths λ_i, can be determined by the phase match condition [14]:

$$\lambda_i = \left(n_{eff}^{co} - n_{eff}^{i,clad}\right)\Lambda, \tag{1}$$

where Λ is the period of the grating, n_{eff}^{co} is the effective refractive index of core mode and $n_{eff}^{i,clad}$ is the effective refractive index of the ith cladding mode.

The strain characteristics of the grating can be determined from Eq. (1) [15]:

$$\frac{d\lambda_i}{d\varepsilon} = \Lambda\frac{d\lambda_i}{d\Lambda}\left(1 + \frac{\eta_{co}n_{eff}^{co} - \eta_{clad}n_{eff}^{i,clad}}{n_{eff}^{co} - n_{eff}^{i,clad}}\right), \tag{2}$$

where η_{co} and η_{clad} are the elastic–optic coefficients of the core and cladding of the fiber, respectively. Thus, when the sensing structure is subjected to strain, the grating period and the effective refractive indices of fiber core and cladding change. Consequently, the variation of these parameters affects the original resonance condition, which is determined by Eq. (1), and modifies the transmission spectrum of the LPFG.

We fabricated the LPFG using the electric arc discharge (EAD) technique [16]. The grating sensor was inscribed in a single-mode fiber with arc power of 70 bits, arc time of 500 ms, grating period of $\Lambda = 500$ µm and length of 30 mm. The transmission spectrum of the LPFG was monitored using an Optical Spectrum Analyzer (OSA) from Anritsu (MS9740A). Figure 1 illustrates the microscopic photograph of the LPFG. It is possible to observe a representation of the grating period, which is based on the position of two electric arc discharges produced in sequence in the optical fiber during the EAD fabrication process.

After the fabrication of the LPFG sensor, we used a commercially available 3D printer (MakerBot Replicator Z18) to embed the LPFG into a 3D-printed polymer structure. Figure 2 shows the design and the photograph of the 3D-printing packaged LPFG. The polylactic acid (PLA) was the raw material used on the printing and the sensor was designed based on a thin and flexible structure having a rectangular shape. The dimension of the printed structure is 3, 10 and 100 mm (height × width × length). In what concerns the 3D printing process, the LPFG sensor was embedded directly

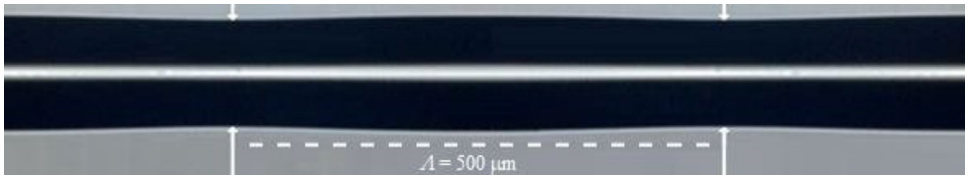

Fig. 1 LPFG fabricated using electric arc discharge technique

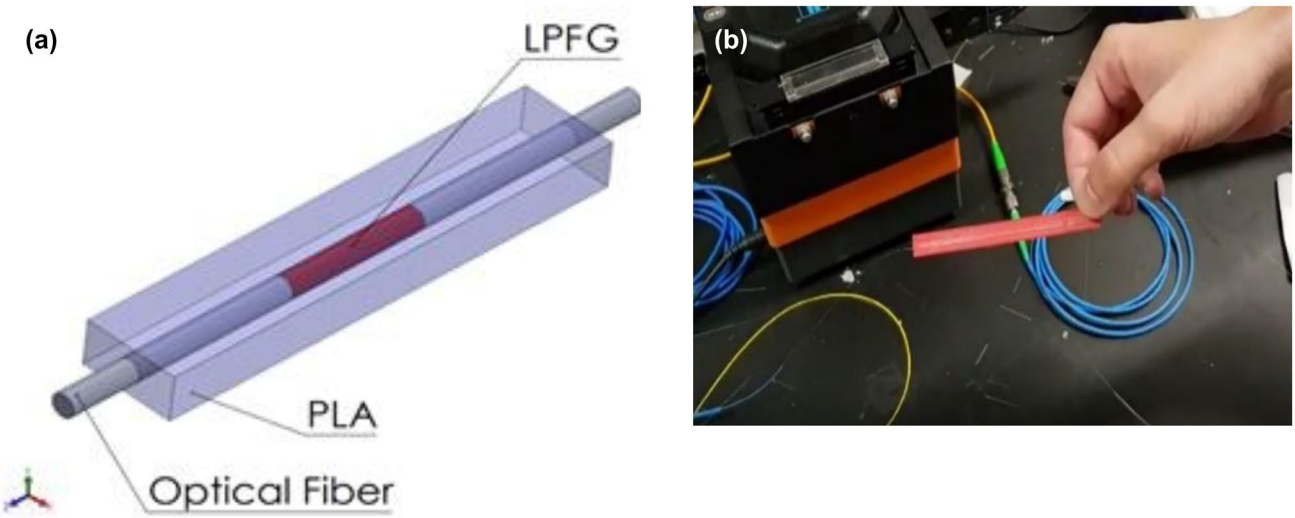

Fig. 2 **a** Design and **b** fabricated LPG-embedded sensor

into PLA plastic in the center of the three-dimensional structure when 50% of its printing process was completed. After that, the injection of hot PLA layer-upon-layer was restarted to complete the printing process. It is important to mention that during the fabrication, we applied a prestress to maintain the LPFG under constant straining state.

3 Results

The LPFG spectra after and before embedded in the thin and flexible PLA structure are shown in Fig. 3. After the fabrication process, the resonant wavelength, which was initially located at 1530 nm, shifted in approximately $\Delta\lambda = 8$–1522 nm. This wavelength shift is attributed to the strain acting on the LPFG positioned inside the structure. Furthermore, the LPFG is sensitive to the surrounding refractive index (RI) [17–19]. Thus, the external RI change caused by the polymer is responsible for the wavelength shift observed after the packaging process, as well as the strain acting on the LPFG caused by the introduction of prestress during the fabrication process.

We have simulated the phase-matching curves for the fabricated LPFG using OptiGrating v. 4.2 software by Optiwave, which can be observed in Fig. 4. Therefore, it is possible to identify the energy coupling between the core and cladding mode located at 1530 nm. In our simulations, we considered a single-mode fiber with core and cladding refractive indices of 1.4492 and 1.444, respectively, and core and cladding diameters of 8.2 and 125 µm, respectively. Figure 4 illustrates the dependence between the grating modulation period and the resonant wavelengths of the $LP_{01} - LP_{05}$ symmetric cladding modes and the black dots correspond

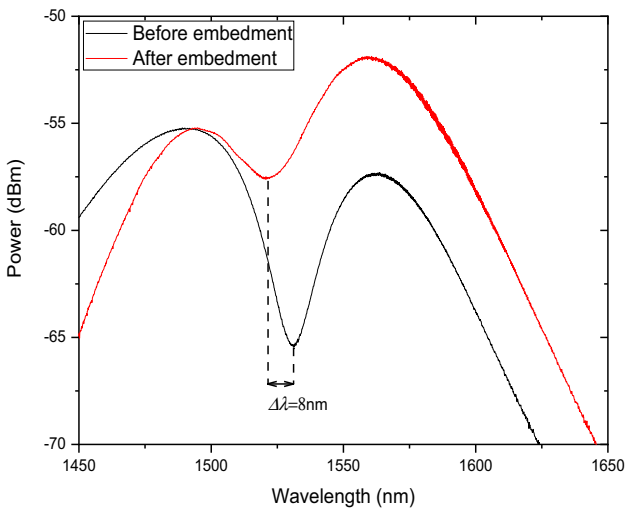

Fig. 3 Transmission spectrum of the LPFG before and after the PLA embedment

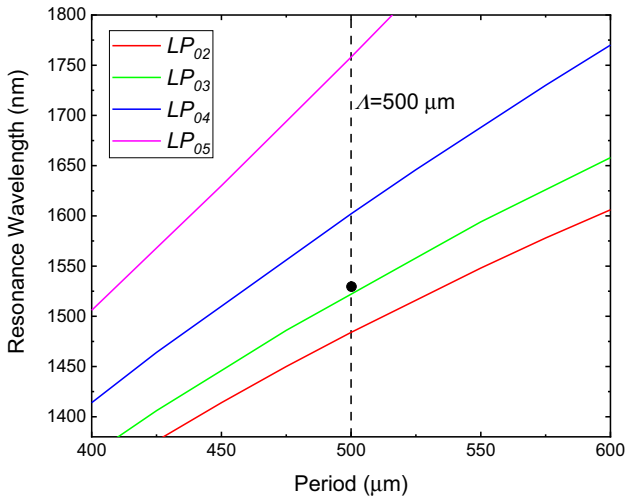

Fig. 4 Simulation of the phase-matching curves

to the experimental data from the produced LPFG with $\Lambda = 500$ µm. For operation near 1550 nm, there is only one coincidence point with the phase-matching curves and provides an indication that the attenuation dip located at 1530 nm, which can be observed in Fig. 3, corresponds to the energy coupling between the fundamental core mode LP_{01} and the LP_{03} cladding mode.

To analyze the strain sensitivity of the LPFG-embedded sensor, we investigated the impact of applied strain on the transmission spectrum of the sensor. For comparison purposes, we also tested the LPFG without the polymer structure. We used a broadband source centered at 1550 nm and an optical spectrum analyzer to acquire and analyze the output data from the sensor. In our experimental tests, the strain was applied with the help of a translation stage and the tests were performed under constant room temperature in an isolated laboratory. Therefore, the strain response of the sensor was measured by clamping one side of the structure to an immobilized support and the other one to the translation stage. The deformation applied in the packaged LPFG varied from 0 to 1000 µε in steps of 200 µε. When straining the sensor, changes in the geometry of the sensing structure occur. Therefore, varying the period of the grating. During the experimental tests, we applied only tensile force on the sensor and no compressive force was exerted.

Figure 5 shows the results for the unembedded grating and the PLA-embedded LPFG. We can observe that the resonant wavelength of both sensors shifted continuously in the direction of shorter wavelengths of the spectrum as the strain increased. Moreover, it was found that the strain response of the tested sensors varied monotonically and linearly and by experimental data fitting with a linear regression approach. Therefore, the unembedded LPFG showed a sensitivity of $S_{LPFG} = -1.5$ pm/µε with high

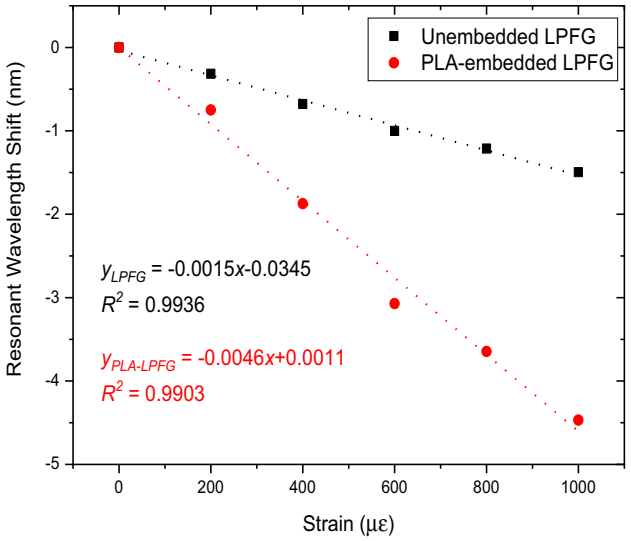

Fig. 5 Resonant wavelength shift as a function of applied strain

degree of strain linearity, confirmed by the R^2 coefficient of 0.9936 derived from the fitting process. On the other hand, the experimental data fitting of the PLA-embedded LPFG resulted in an enhanced sensitivity of $S_{PLA-LPFG} = -4.6$ pm/με with a R^2 coefficient value of 0.9903 over the strain sensing range, as observed in Fig. 5. These results indicate that the strain sensitivity of the PLA-embedded LPFG is higher than that of a traditional LPFG [20]. This enhanced sensitivity is related to a higher strain that is transmitted to the LPFG due to the stiffness that the infill density provides when compared to the unembedded grating. Therefore, the PLA patch has the function of improving the strain transfer and acts as gaining factor on the deformation sensitivity of the LPFG sensor. It should be also remarked that the sensor performance can be further improved. The main possibility to enhance the strain sensitivity could be, for example, the coupling to higher-order cladding modes, since the sensing behavior is dependent on mode order.

We emphasize that accurate wavelength demodulation can be achieved at low contrast ratio. For example, Mahakud et al. [21] reported experimental results and analysis based on wavelength demodulation at low contrast ratio for resonant modes of a LPFG sensor. Finally, it is important to mention that LPFG sensors with higher contrast ratio (> 10 dB) can be fabricated using the electric arc discharge method. For instance, the arc power may increase the contrast ratio of the resonant modes, which enables the fabrication of more competitive strain sensors. Thus, this particular topic will be discussed in detail in future work.

To give a wider perspective, Table 1 lists the strain sensitivities obtained in the present study in comparison with conventional and other different configurations of strain sensors based on fiber gratings. It is important to mention that we considered different configurations of fiber grating sensors operating within similar strain ranges. Moreover, it is observed in Table 1 for the LPFGs the resonant wavelength of the cladding modes decreases with strain applied on the sensor, which results in a negative sensitivity. This behavior is related to the dependence of the resonance wavelength shift of the LPFGs on both the grating period and the refractive index perturbation [22], as indicated in Eq. (2).

Table 1 Comparison between different configurations of fiber grating sensors

Type	Strain sensitivity (pm/με)	Reference
LPFG (ours)	− 1.5	This work
PLA-embedded LPFG (ours)	− 4.6	This work
LPFG 1	− 0.5	[20]
LPFG 2	− 0.82	[23]
LPFG in polarization-maintaining Panda fiber	− 1.82	[24]
FBG	0.706	[13]
PLA-embedded FBG	1.08	[13]
TPU half-embedded FBG	1.40	[25]

4 Conclusion

In this work, a novel 3D-printed LPFG sensor was successfully designed and fabricated using PLA polymer material. This fabrication method is characterized by the advantages of fast, flexible and easily customizable fabrication process and protection of the sensor. The results indicate that it is possible to produce strain sensors with higher sensitivity than the conventional LPFGs found in literature. Furthermore, the enhanced strain sensitivity is an advantage over the embedded FBGs, which was not observed until now. Moreover, considering the dependence of the resonant wavelength shift to external parameters, we believe that this embedded LPFG could be used to enable multiparameter sensing, as well as to explore the possibility of multiplexing. Finally, these advantages could be used to promote the development of novel strain optical fiber sensing applications.

Acknowledgements This work was supported by Coordenação de Aperfeiçoamento de Pessoal de Nível Superior (CAPES), Conselho Nacional de Desenvolvimento Científico e Tecnológico (CNPq) and Instituto Nacional de Energia Elétrica (INERGE) through the Electrical Engineering Graduate Program (PPEE) funds at Federal University of Juiz de Fora (UFJF).

References

1. F. Chiavaioli, F. Baldini, C. Trono, Fibers **5**(3), 29 (2017)
2. C. Hong, Y. Zhang, D. Su, Z. Yin, IEEE Access **7**, 107154 (2019)
3. R. Lima, R. Tavares, S.O. Silva, P. Abreu, M.T. Restivo, O. Frazão, Proc. SPIE **10323**, 103233 (2017)
4. H.A. Dinovitzer, A. Laronche, J. Albert, IEEE Sens. J. **19**(14), 5670 (2019)
5. B. Berman, Bus. Horiz. **55**(2), 155 (2012)
6. T.D. Ngo, A. Kashani, G. Imbalzano, K.T.Q. Nguyen, D. Hui, Compos. B Eng. **143**, 172 (2018)
7. A. Leal-Junior, J. Casas, C. Marques, M. Pontes, A. Frizera, Sensors **18**(12), 4120 (2018)
8. Y.-F. Zhang, C.-Y. Hong, R. Ahmed, Z. Ahmed, Measurement **112**, 74 (2012)
9. Y. Yang, C. Hong, Z.A. Abro, L. Wang, Z. Yifan, Sens. Actuators, A **295**, 663 (2019)
10. C. Hong, Y. Zhang, L. Borana, IEEE Access **7**, 38577 (2019)
11. L. Fang, T. Chen, R. Li, S. Liu, IEEE Sens. J. **16**(17), 6604 (2016)
12. A.G. Leal-Junior, C. Marques, M.R.N. Ribeiro, M.J. Pontes, A. Frizera, IEEE Sens. J. **18**(20), 8381 (2018)
13. W. Yan, S. Ma, H. Wang, X. Zhang, Opt. Laser Technol. **131**, 106443 (2020)
14. S.W. James, R.P.J.M.S. Tatam, Measur. Sci. Technol. **14**(5), 49 (2003)
15. Y. Zhang, P. Jiang, D. Qiao, Y. Xi, Y. Zhu, Q. Xu, C. Wang, Opt. Laser Technol. **21**, 105839 (2020)
16. F.S. Delgado, A. Bessa dos Santos, Opt. Eng. **57**(6), 067105 (2018)
17. H. Tsuda, K. Urabe, Sensors **9**(6), 4559 (2009)
18. B.H. Lee, Y. Liu, S.B. Lee, S.S. Choi, J.N. Jang, Opt. Lett. **22**, 1769 (1997)
19. M. Śmietana, M. Dominik, P. Mikulic, W.J. Bock, Opt. Laser Technol. **107**, 268 (2018)
20. F. Esposito, A. Srivastava, S. Campopiano, A. Iadicicco, Proceedings **15**(1), 29 (2019)
21. R. Mahakud, J. Kumar, O. Prakash, S.K. Dixit, Appl. Phys. B **126**, 90 (2020)
22. G. Chen, H. Xiao, Y. Huang, Z. Zhou, Y. Zhang, Proc. SPIE **7292**, 729212 (2009)
23. A. Iadicicco, S. Campopiano, Sensors **15**(4), 8009 (2015)
24. R. Ranjan, F. Esposito, S. Campopiano, A. Iadicicco, IEEE Sens. J. **17**(21), 6953 (2017)
25. A.G. Leal-Junior, C. Díaz, C. Marques, A. Frizera, M.J. Pontes, Sensors **19**, 3514 (2019)